THE JOURNAL OF BIOLOGICAL CHEMISTRY VOL. 291, NO. 15, pp. 8199–8213, April 8, 2016

GSK3β Overexpression in Dentate Gyrus Neural Precursor Cells Expands the Progenitor Pool and Enhances Memory Skills*

Received for publication, July 3, 2015, and in revised form, February 4, 2016 Published, JBC Papers in Press, February 17, 2016, DOI 10.1074/jbc.M115.674531

Jerónimo Jurado-Arjona[‡§], **María Llorens-Martín**[‡§], **Jesús Ávila**[‡§], **and Félix Hernández**[‡§1]

From the [‡]*Centro de Biología Molecular "Severo Ochoa," Consejo Superior de Investigaciones Científicas/Universidad Autónoma de Madrid (CSIC/UAM), Cantoblanco, 28049 Madrid, Spain and the* [§]*Centro de Investigación Biomédica en Red de Enfermedades Neurodegenerativas (CIBERNED), 28031 Madrid, Spain*

In restricted areas of the adult brain, like the subgranular zone of the dentate gyrus (DG), there is continuous production of new neurons. This process, named adult neurogenesis, is involved in important cognitive functions such as memory and learning. It requires the presence of newborn neurons that arise from neuronal stem cells, which divide and differentiate through successive stages in adulthood. In this work, we demonstrate that overexpression of glycogen synthase kinase (GSK) 3β in neural precursor cells (NPCs) using the glial fibrillary acidic protein promoter during DG development produces an increase in the neurogenic process, increasing NPCs numbers. Moreover, the transgenic mice show higher DG volume and increased number of mature granule neurons. In an attempt to compensate for these alterations, glial fibrillary acidic protein/GSK3β-overexpressing mice show increased levels of Dkk1 and sFRP3, two inhibitors of the Wnt-frizzled complex. We have also found behavioral differences between wild type and transgenic mice, indicating a higher rating in memory tasks for GSK3β-overexpressing mice compared with wild type mice. These data indicate that GSK3β is a crucial kinase in NPC physiology and suggest that this molecule plays a key role in the correct development of DG and adult neurogenesis in this region.

Adult neurogenesis is the production of new neurons not only during development but throughout life. It has been described in many mammalian species, including human (1). This process mainly takes place in two brain regions: the subventricular zone at the lateral ventricle (2) and the subgranular zone (SGZ)[2] in the dentate gyrus (DG) at the hippocampus (3). In both regions there are neural stem cells that divide to reach, at the end of the process, a mature newborn neuron. These precursors have an astrocyte-like phenotype expressing the glial fibrillary acidic protein (GFAP) (4, 5).

DG is a discrete structure that is postnatally developed (6). After birth, the first granule neurons are formed in the hippocampal neuroepithelium and move to form a DG primordium. Afterward, granule precursor cells, also from this area, migrate to the primordium. These mitotic cells form a germinal matrix that gives rise to an adult DG after 1 month of life (7, 8). After finishing the formation, some neural precursor cells remain in the SGZ dividing and constantly generating newborn granule neurons (9), which connect with the preexistent trisynaptic circuit of the hippocampus (10). Newborn granule neurons have a major role in hippocampus-dependent memory and learning tasks and in anxiety and depression (11).

For these reasons, understanding neural precursor cell proliferation and differentiation and adult neurogenesis is an important goal. GSK3 is a kinase that has been postulated as an important player in this process (12–15). GSK3 is a serine-threonine kinase with two highly conserved isoforms, α and β. GSK3β has a pivotal role in neurodevelopment, regulating different processes such as neuronal polarity, axonal outgrowth, migration, apoptosis, neurotransmission, synaptic development, and plasticity (16, 17).

Some evidence about the importance of GSK3 in neurogenesis comes from genetically modified models. In this sense, the loss of DISC1 (*disrupted in schizophrenia 1*), a GSK3 inhibitor by protein interaction, promotes a decrease in neural precursor cells (NPCs) proliferation and an increase in differentiation, which is overridden using GSK3 inhibitors (18). Furthermore, in double knock-in mice with constitutive active GSK3, by the mutation of the phosphorylated inhibitory serines 21 and 9 to alanines in both GSK3α/β isoforms, a decrease in NPC proliferation was detected (12). The opposite phenotype is observed in knock-out embryos of both GSK3 isoforms in NPCs nestin+ (13). However, some findings related to GSK3 functions in NPCs are controversial. For instance, the growth of the NPCs depends of the levels of GSK3 inhibition (19).

NPCs progressively generate more differentiated progeny, which eventually mature into granule neurons. Thus, the role of GSK3β in adult neurogenesis should be analyzed step by step. In previous reports, we found that an overexpression of the kinase in later stages of neurogenesis from DCX cells to mature neurons has negative consequences for the neurogenic process (14, 20). However, the direct role of GSK3β overexpression in

* This work was supported in part by Ministerio de Educación y Ciencia Grants SAF2011-24841 and BUF2013-40664-P, Comunidad de Madrid Grant S2010/BMD-2331, and funds from the Fundación Ramón Areces. The authors declare that they have no conflicts of interest with the contents of this article.

[1] To whom correspondence should be addressed: Centro de Biología Molecular "Severo Ochoa," CSIC/UAM, Universidad Autónoma de Madrid, Cantoblanco, 28049 Madrid, Spain. Tel.: 34-91-196-45-63; Fax: 34-91-196-44-20; E-mail: fhernandez@cbm.csic.es.

[2] The abbreviations used are: SGZ, subgranular zone; DG, dentate gyrus; GFAP, glial fibrillary acidic protein; NPC, neural precursor cell; GSK, glycogen synthase kinase; DCX, Doublecortin; CldU, 5-chloro-2′-deoxy-uridine; IdU, 5-iodo-2′-deoxy-uridine; tTa, tetracycline-regulated transactivator; BLBP, brain lipid-binding protein; P*n*, postnatal day *n*.

the first step of the process *in vivo*, just in NPCs, has not been addressed so far.

Here, we further studied the consequences of *in vivo* GSK3β overexpression in NPCs using the GFAP promoter on adult hippocampal neurogenesis, having in mind the possible effect during DG formation. An increase in the number of NPCs, as well as in the total number of mature granule neurons and DG volume, was observed. However, these effects are not only due to adult neurogenesis but are also attributable to the overexpression during DG development. This atypical environment is controlled and retained to avoid a higher increase in neurogenesis by high levels of Wnt inhibitor pathway. Overall, the alterations of all these parameters change the behavior of these GFAP/GSK3 transgenic mice, increasing their memory skills.

Experimental Procedures

Animals

Mice were bred at the Centro de Biología Molecular "Severo Ochoa" animal facility, under standard laboratory conditions in accordance with European Community Guidelines and handled in accordance with European and local animal care protocols. The mice were housed 4–5/cage with food and water available *ad libitum* and maintained in a temperature-controlled environment on a 12/12-h light/dark cycle with light onset at 8 a.m.

The studies in adult neurogenesis were done with GFAP/GSK3β double transgenic, with all experimental procedures authorized by the Bioethics Committee of Centro de Biología Molecular Severo Ochoa (Universidad Autónoma de Madrid-Consejo Superior de Investigaciones Científicas, UAM-CSIC, Madrid, Spain). GFAP/GSK3β mice were obtained by crossing Bi-TetO β-gal GSK3β mice (21) (carrying the bidirectional Tet-responsive promoter followed by GSK3β and β-galactosidase cDNAs, one in each direction) with GFAP-tTa mice (Jackson Laboratory; B6.Cg-Tg(GFAP-tTa)110Pop/J no. 005964). WT animals resulting from crossing GFAP-tTa line with C57/BL6 mice were used as a control group. All experiments were conducted in animals 3.5 months old, except those shown in Fig. 7 and Table 1.

Tissue Processing

The mice were fully anesthetized with an intraperitoneal pentobarbital injection (Dolethal, 60 mg/kg body weight) and transcardially perfused with saline 0.9% followed by 4% paraformaldehyde in phosphate buffer. The brains were removed and postfixed overnight in 4% paraformaldehyde. For immunofluorescence experiments, 50-μm-thick sagittal brain sections were obtained on a Leica VT1200S vibratome.

The animals used for biochemical analysis were fully anesthetized with an intraperitoneal pentobarbital injection and transcardially perfused just with saline. The brains were removed, and the hippocampi were quickly dissected on ice and frozen in liquid nitrogen.

Immunofluorescence

For immunofluorescence, a series of brain slices were made up randomly of one section from every nine. Slices were initially preincubated in phosphate buffer with 1% Triton X-100 and 1% BSA. Then sections were incubated for 48 h at 4 °C using the following primary antibodies: mouse anti-β-galactosidase (1:5000 Promega, catalog no. Z378A, lot 18637309) chicken anti-β-galactosidase (1:5000, Abcam, catalog no. ab134435, lot GR105546-10); mouse anti-cMyc (1:100, Roche, catalog no. 11 667 203 001, lot 10138400), rabbit anti-BLBP (1:400, Abcam, catalog no. ab32423, lot GR165246–1), goat anti-Sox2 (1:500, R&D Systems, catalog no. AF2018, lot KOY0112011); rabbit anti-GFAP (1:500, Promega, catalog no. G560A, lot 11173502); mouse anti-GFAP (1:500, Calbiochem, catalog no. IF03L, lot D00132185); rabbit anti-S100β (1:500, Dako, catalog no. Z0311, lot 20025982), polyclonal rabbit anti-nuclear Ki-67 (1:500, Novocastra-Leica, catalog no. NCL-L-ki67-MM1, lot 6027899); goat anti-Doublecortin (DCX) (1:500, Santa Cruz, catalog no. sc-8066, lot G0413); rabbit anti-NeuN (1:1000, Millipore, catalog no. ABN78, lot 2110559); rabbit anti-PHisH3 (1:250 Millipore catalog no. 06–570, lot 2202541); rabbit anti-Calbindin (1:500, Swant, catalog no. CB38a, lot 9.03); rabbit anti-fractin (1:500, BD Pharmingen, catalog no. 551527, lot 81106E); rat anti-BrdU/CldU (1:400, Accurate Chemical & Scientific Corporation, catalog no. OBT0030S, lot J0031); and mouse anti-IdU (1:500, BD Biosciences, catalog no. 347580, lot 2346657). The binding of these antibodies was detected by incubating for 24 h at 4 °C with the appropriate donkey Alexa-conjugated secondary antibodies (1:1000, Molecular Probes). All the sections were finally counterstained for 10 min with DAPI (1:10,000, Calbiochem).

When the immunofluorescence was perform to detect thymidine analogs, a preincubation of 30 min with 2 N HCl was performed. Then sections were gently washed in phosphate buffer following the described protocol.

Western Blotting Analysis

Extracts for Western blotting analysis were prepared by homogenizing the sample tissue in ice-cold extraction buffer consisting of 50 mM Tris-HCl, pH 7.4, 150 mM NaCl, 1% Nonidet P-40, 1 mM sodium orthovanadate, 1 mM EDTA, a protease inhibitor mixture COMPLETE™ (Roche), and 1 μM okadaic acid. The samples were homogenized, and protein content was determined by the Bradford method. Twenty micrograms of total protein were electrophoresed on 10% SDS-polyacrylamide gel and transferred to a nitrocellulose membrane (Schleicher & Schuell). Prior to antibody hybridation, membranes were blocked with 5% nonfat dried milk. The following primary antibodies were used: mouse anti-β-galactosidase (1:5000 Promega, catalog no. Z378A, lot 18637309); rabbit anti-GFAP (1:1000 Promega, catalog no. G560A, lot 11173502); and mouse anti-β-actin (1:5000 Sigma, catalog no. A5441, lot 014M4759). The membranes were incubated with the antibody at 4 °C overnight in the same blocking solution. Secondary goat anti-mouse and anti-rabbit antibody (1:5000; Dako) conjugates with HRP and ECL detection reagents (Amersham Biosciences) were used for immunodetection.

Injection of Thymidine Analogs

5-Chloro-2′-deoxy-uridine (CldU, 57.65 mg/kg intraperitoneal; Sigma-Aldrich) and 5-iodo-2′-deoxy-uridine (IdU, 42.75

mg/kg intraperitoneal; Sigma-Aldrich) were administered to animals at different time points (4 weeks, 1 week, or 24 h prior to sacrifice). For every time point, the animals were injected once. IdU and CldU doses were based on equimolar doses of 50 mg/kg BrdU as previously described (22).

Dentate Gyrus Volume

The volume of the dentate gyrus was estimated stereologically by applying the Cavalieri method to each series of Nissl-stained sections, as described previously (23). DG areas were measured in each slice of the series using ImageJ software (version 1.33; National Institutes of Health, Bethesda, MD).

Cell Counting

The total number of precursor cells BLBP+, Sox2+, immature neurons DCX+, and cells in mitosis in P14 mice (PHisH+) were calculated using the physical dissector method adapted for confocal microscopy as described elsewhere (23). Confocal stacks of images were obtained using a LSM710 Zeiss confocal microscope with a 63× oil immersion objective. Four stacks of images were analyzed per animal.

Total number of positive cells for the markers IdU, CldU, and fractin were quantified under an inverted Axiovert200 Zeiss fluorescence microscope (×40 oil immersion objective), using the optical dissector method (23). Briefly, using series composed of every eighth section, the cells labeled for each marker in every section were counted, and the total number of cells counted was then multiplied by 8 to obtain the total number of cells in the whole DG.

Colocalization studies of IdU+ (12 h) with CldU+ (2 h) analyzed a sufficient number of IdU+ cells (1000 cells per genotype obtained from a representative number of animals from each group) and classifying them as negative or positive for the other marker. In the case of colocalization studies with IdU+ (4 weeks), all cells positive for thymidine analog were analyzed for different maturation steps markers (DCX or Calbindin). Data are shown as percentages relative to the total number of IdU+ cells. Total mature granule neurons was analyzed through the application of a physical dissector method developed for confocal microscopy (Zeiss LSM710) 100× oil immersion objective.

Quantitative PCR

The hippocampus from one hemisphere of each animal was used to isolate total RNA with the QIAzol lysis reagent (Qiagen) and RNeasy mini kit (Qiagen). The samples were homogenized in TissueLyser II with stainless steel beads (5 mm). Reverse transcription was performed using the high capacity cDNA reverse transcription kit (Applied Biosystems) in a final RNA concentration of 20 ng/μl. Quantitative PCR was developed on a LightCycler 480 (Roche Applied Science) (384 multiwell plates). 5 ng of cDNA/well was run in triplicate. A final volume of 10 μl in each well was prepared with the following concentrations: primers (250 nM concentration), Universal Probe Library Probes (100 nM), and LightCycler 480 Probes Mastermix (2×) (Roche Applied Science). Data from each gene was normalized by 18S ribosomal gene as control. The following Universal Probe Library gene-specific primers were used: DKK1 (forward, CCGGGAACTACTGCAAAAAT; reverse, CCAAGGTTTTCAATGATGCTT), sFRP3 (forward: CACCGTCAATCTTTATACCACCT; reverse: TCAGCTATAGAGCCTTCTACCAAGA), and Rn18s (forward: CGGCTACCACATCCAAGGAA; reverse: GCTGGAATTACCGCGGCT) as endogenous control.

Behavioral Studies

Open Field—Major locomotor activity was measured in clear Plexiglas boxes measuring 43.2 cm × 43.2 cm outfitted with photobeam detectors for monitoring horizontal and vertical activity. Activity levels were recorded with an activity monitor (MED Associates, St. Albans, VT). Locomotor activity data were collected via PC and analyzed with the MED Associates activity monitor data analysis software. The mice were placed in a corner of the open field apparatus and left to move freely. The variables recorded included: vertical counts, jumps, and average velocity (cm/s). The data were individually recorded for each animal for 15 min.

Fear Conditioning Test—A special system for fear conditioning (Panlab) was used. It consists of a box of sound attenuation. The floor, which detects any mouse movements, was made of stainless steel rods connected to a shock delivery apparatus. Inside the box, there was a loudspeaker to emit acoustic stimuli of known intensity, frequency, and duration to the experimental subjects. The apparatus was connected to a stimulus programming device to predetermine number, duration, and rate of sound and electric shock.

For conditioning phase, mouse was placed inside the conditioning apparatus. The 6-min protocol consisted of allowing the mouse 3 min for exploration. After this time, there were two cycles of acoustic stimuli lasting 30 s followed by 2 s of 0.8-mA electric foot shock; the cycles were separated by 1 min. As a control, animals from both genotypes were conditioned with the same protocol removing the electric shock after the acoustic stimuli. 24 h later, conditioned freezing was measured. The animals were again placed inside the conditioning apparatus and left there for 6 min. While they were there, neither electrical nor acoustic stimuli were administered. Freezing time was measured with a PC and was analyzed with Freezing v1.3.03 software. The control animals did not show freezing, demonstrating that neither the cage nor the acoustic stimulus produce an aversive conditioning.

Statistical Analysis

The data are presented as mean values ± S.E. Statistical analyses of data were performed by applying a Student's *t* test for each statistical comparison. $p < 0.05$ values were considered significant. An Mann-Whitney *U* test was used when a nonparametric test was required. All statistics were analyzed using SPSS 17.0.1 software (SPSS, 1989; Apache Software Foundation).

Results

Mouse Design to Overexpress GSK3β in Neural Precursors—To analyze the role of GSK3β in NPCs, we have generated transgenic mice where GSK3β overexpression is driven by a GFAP promoter (GFAP/GSK3β mice; Fig. 1*A*). To this aim, we have used GSK3β transgenic mice (Bi-TetO GSK3β), which

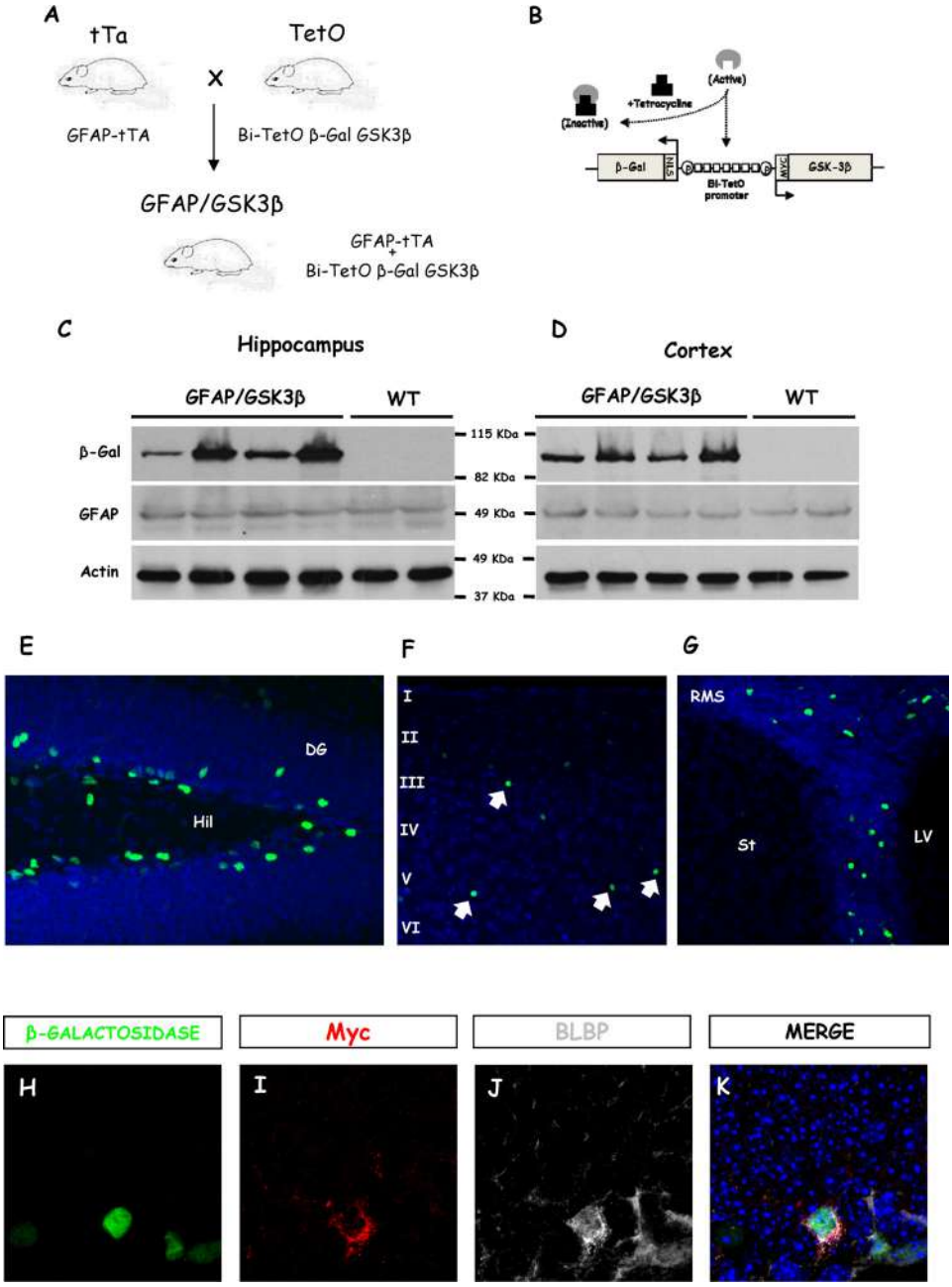

FIGURE 1. **Generation and pattern of transgene expression in GFAP/GSK3β.** *A*, generation of conditional double transgenic mice GFAP/GSK3β is achieved by breeding Bi-TetO GSK-3β mice, carrying GSK3β transgene, with GFAP-tTa mice expressing tTa under control of a truncated GFAP promoter. *B*, diagram representation of GSK3β transgene activation. Bi-TetO promoter is formed by seven copies of the palindromic tet operator sequence containing two cytomegalovirus minimal promoter sequences (*P*), one in each end, in divergent orientations. This bidirectional promoter is followed by a GSK3β cDNA sequence (fused with a myc epitope at its 5′-end) in one direction and β-galactosidase (LacZ) sequence encoding a nuclear localization signal in the other. The minimal promoter is active, and therefore the transgene is expressed only when it has joined the transactivator. This allows muting the expression with tetracycline administration. *C* and *D*, Western blotting detection of transgene expression using β-gal antibody in hippocampus (*C*) and cortex (*D*) of GFAP/GSK3β mice and WT mice. Actin and GFAP has been used as a load control. Lines show molecular masses in kDa. *E–G*, β-Galactosidase immunofluorescence on sagittal brain sections from GFAP/GSK3β mice, showing DG (*E*), cortex (*F*), and subventricular zone (*G*). The *white arrows* in *F* show mature astrocytes positive for β-gal. *H–K*, triple immunofluorescence showing a β-gal-positive cell (*H*) which also express myc epitope corresponding to transgenic GSK3β (*I*). As expected, this cell is a neural precursor cell, positive for BLBP marker (*J*). *K* shows merge of all channels. *DG*, dentate gyrus; *Hil*, hilus; *I–VI*, cortical layers; *LV*, lateral ventricle; *St*, striatum; *RMS*, rostral migratory stream.

were generated in our laboratory as previously described (21). Briefly, these transgenic mice carry a bidirectional TetO promoter (Bi-TetO) followed by GSK3β cDNA encoding in 5′ a myc epitope in one direction and a β-galactosidase (β-Gal) reporter gene fused with a nuclear location signal in the other (Fig. 1*B*). The GFAP/GSK3β mice derive from crossing homozygous Bi-TetO GSK3β and GFAP-tTa lines (Fig. 1*A*). The last one (24) carries a tTa under a truncated GFAP promoter, so the double transgenic progeny are expected to overexpress GSK3β in GFAP-positive cells, such as NPCs. GFAP/GSK3β transgenic mice were viable, had a normal lifespan, and grew normally. The percentage of each

genotype in the littermates was the expected Mendelian frequency of 50%.

Pattern of Transgene Expression—First, we checked the pattern of transgene expression in hippocampus and cortex by Western blotting and immunofluorescence (Fig. 1, *C*, *D*, and *E–G*). When GFAP/GSK3β mice were analyzed by Western blotting, β-Gal reporter protein was detected in the double transgenic mice (GFAP/GSK3β) in hippocampus (Fig. 1 C) and cortex (Fig. 1*D*). No β-gal expression was observed in wild type mice (Fig. 1, *C* and *D*). Probing protein extracts with anti-myc (which label the N-terminal end of transgenic kinase) and anti-GSK3β antibodies we did not observe any increase in GSK3β levels in the hippocampal or cortical samples, demonstrating that few cells show transgenic GSK3β expression (data not shown).

Immunofluorescence analysis of GFAP/GSK3β mice brain sections showed restricted region expression. More precisely, the expression of the transgene takes place in the two brain regions with adult neurogenesis: in DG (Fig. 1*E*) in the SGZ of the hippocampus where neurogenic precursors are located and the subventricular zone at the lateral ventricle (Fig. 1*G*). In cortex, a reduced expression was essentially taking place in astrocytes (Fig. 1*F*). No β-gal expression was detected in striatum or brainstem (not shown). To gain insight into which cell populations overexpress GSK3β, we performed immunohistochemistry with anti-myc antibody. In the hippocampus, increased immunoreactivity for MYC-GSK3β was restricted to the DG and colabeled with BLBP (Fig. 1, *H–K*). Although β-gal-positive cells were observed in the cortex, no immunoreactivity for MYC-GSK-3β was observed.

GFAP/GSK3β Mice Overexpress GSK3β in NPCs of the DG—Taking into account that we are using a bidirectional promoter that allows the expression of GSK3β and the expression of a reporter gene, β-galactosidase, under the control of GFAP promoter, we first analyzed whether the reporter (and consequently transgenic GSK3β) was expressed in NPCs in the dentate gyrus (DG) of the hippocampus. For this aim, we performed double immunofluorescence experiments against β-gal and GFAP protein (Fig. 2, *A–E*). Cells overexpressing GSK3β were in the correct SGZ location, and a characteristic GFAP apical process was found (*white arrow*). In addition, other cell types positive for GFAP were located in the hippocampus and also express the transgene (*white arrowhead*). To demonstrate that these cells are astrocytes, we used S100β, a molecular marker of mature astrocytes that does not label radial astrocytes acting as neurogenic progenitors. Fig. 2 (*F–K*) shows triple immunolabeling for GFAP, β-galactosidase, and S100β. *White arrows* show a NPCs located in the SGZ, positive for β-galactosidase and negative for S100β and with GFAP apical processes penetrating the GCL. The *white arrowhead* shows a double positive non-neurogenic astrocyte, and the *thin white arrows* show a mature astrocytes in the hilus and in the DG, which do not express the transgene. These data demonstrate that astrocytes do not form a homogeneous population of cells.

To unequivocally confirm the overexpression of GSK3β by NPCs, we perform double immunofluorescence with specific NPCs markers. Thus, brain lipid-binding protein (BLBP, a stage-specific marker for radial glia-like cell) (Fig. 2, *L–P*) and Sox2 (Fig. 2, *Q–U*) confirmed the expression of transgenic GSK3β, detected by β-gal reporter, in adult hippocampal precursor cells.

Adult neurogenesis consists of different stages starting by the proliferation of type B cells (astrocytes) that then differentiate into DCX+ cells and mature turning into functional neurons (11). Thus, we tested the expression of the transgene in the different stages that characterize the process (Fig. 3). Using Ki67 antibody, which labels dividing cells, we demonstrated that β-gal expression colocalizes with Ki67 (Fig. 3, *A–C*). This fact shows that GSK3β transgene expression remains in dividing cells in the SGZ. We also checked a more mature state in the neurogenic process. We used DCX antibody for neuroblast labeling. No colocalization between β-gal protein and DCX was seen (Fig. 3, *D–F*). Finally, we tested whether transgene was expressed in mature granule cells using NeuN antibody. Positive cells for β-gal antibody did not express NeuN marker (Fig. 3, *G–I*). These data suggest that exogenous GSK3β is expressed in dividing cells located in the SGZ and does not remain during the neuron's lifetime.

GFAP/GSK3β Mice Show an Increase in Neural Progenitor Cells, Mature Granule Cells, and Dentate Gyrus Volume—Having demonstrated the expression of transgene in NPCs, we examined the physiological implication of this overexpression. First, we analyzed whether any variation exists in DG volume using the Cavalieri method. The quantification of the total volume showed a significant increase in DG volume of GFAP/GSK3β compared with control mice (Fig. 4, *A–C*). To support this finding, we also measured the number of total mature granule neurons in the DG in each genotype. The quantification demonstrated a higher number of granule neurons in GFAP/GSK3β mice compared with matched control (Fig. 4, *D–F*).

After observing an increase in DG volume and in the number of mature cells, we analyzed whether these changes could be produced by an alteration in NPCs caused by GSK3β overexpression. Using a physical dissector method, we quantified the amount of neural precursor by assessing the number of cells labeled with BLBP (Fig. 5, *A* and *B*) and with Sox2 (Fig. 5, *C* and *D*). With both markers, we have shown an increase in the number of neural precursor cells in GSK3β transgenic mice compared with WT mice (Fig. 5, *G* and *H*). Then we checked what happened with the next differentiated stage of newborn neurons, characterized by expression of DCX (Fig. 5, *E* and *F*). The quantification of DCX positive cells showed, agreeing with previous data, an increase in the number of these cells in GFAP/GSK3β (Fig. 5*I*). These data suggest that increases in the number of NPCs, mature cells, and dentate gyrus volume in transgenic mouse are due to the effect of GSK3β overexpression *in vivo*.

The Increase of Neural Progenitor Cells in GFAP/GSK3β Is Due to GSK3β Overexpression during Development—To go further in these findings, we tested the hypothesis of an increase in proliferation as a reason for the observed neural precursors increase. We carried out the evaluation of proliferation rate by immunolabeling using the antibody anti-phosphohistone H3, a mitotic marker. No statistical differences between the genotypes were noted in NPCs proliferation (data not shown). To rule out that the alteration was at the proliferation level, we

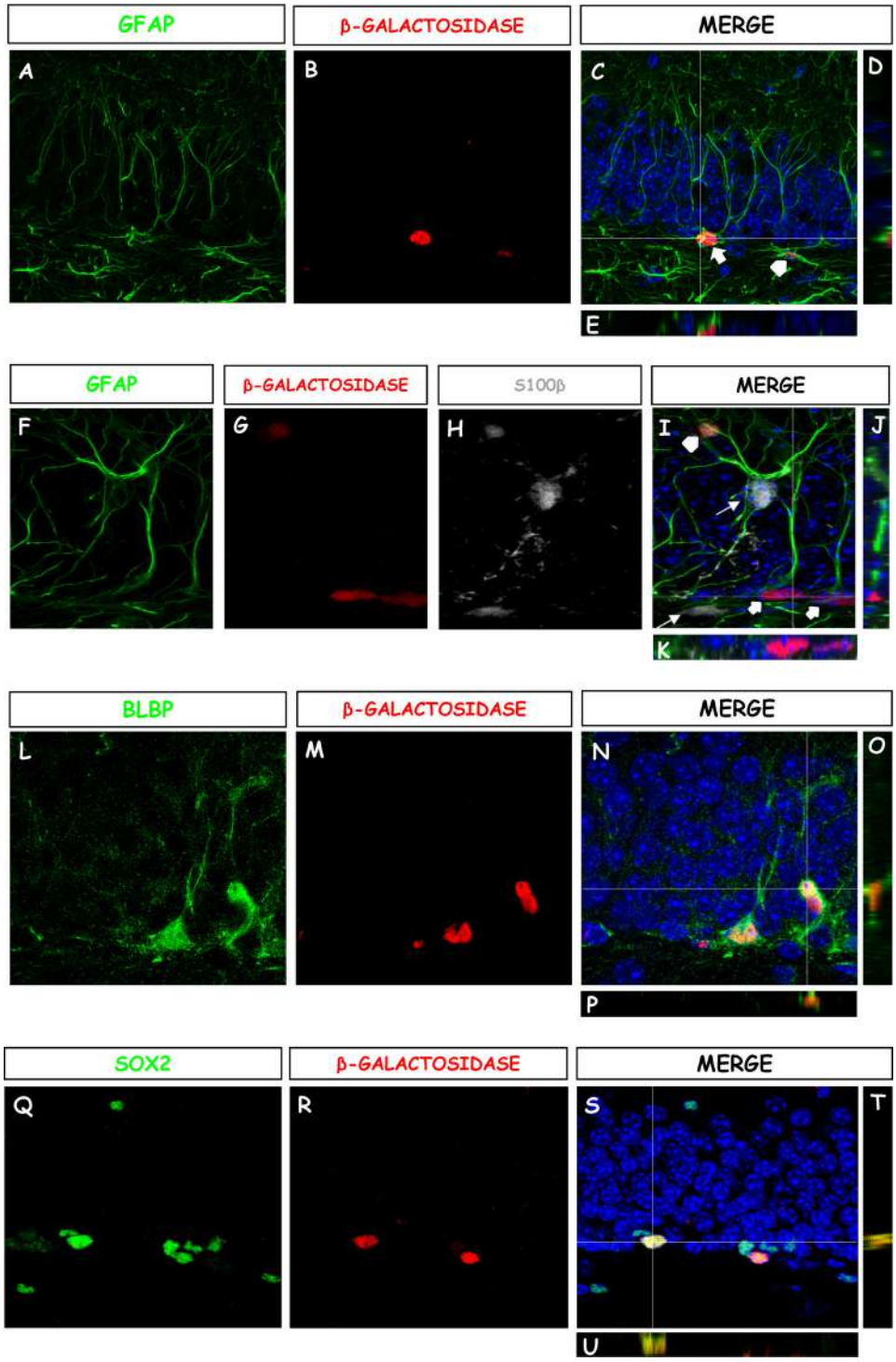

FIGURE 2. **Overexpression of GSK3β in neural progenitors of GFAP/GSK3β.** *A–C*, double immunofluorescence for GFAP (*A*, *green channel*) and β-galactosidase (*B*, *red channel*). *C*, merge panel with granule neurons in DG counterstained with DAPI (*blue channel*). The *white arrow* shows a double positive NPC located in the SGZ. The *white arrowhead* shows a double positive astrocyte in the hilus. *D* and *E*, orthogonal view of double positive NPC, which overexpress GSK3β. *F–I*, triple immunolabeling for GFAP (*F*, *green*), β-galactosidase (*G*, *red*), and S100β (*H*, *gray*). *I*, merge panel with DAPI staining in *blue*. The *white arrows* show a NPCs located in the SGZ, positive for β-galactosidase and negative for S100β. The *white arrowhead* shows a double positive non-neurogenic astrocyte. The *thin white arrows* show a mature astrocytes in the hilus and in the DG, which do not express the transgene. *J* and *K*, orthogonal view of double positive NPC, which overexpress GSK3β. *L–N*, double immunolabeling for BLBP (*L*, *green*) and β-galactosidase (*M*, *red*) in hippocampus of GFAP/GSK3β. *N*, merge panel with DAPI staining in *blue*. *O* and *P*, orthogonal view of double positive NPC, which overexpress GSK3β. *Q–S*, double immunolabeling for Sox2 (*Q*, *green*) and β-galactosidase (*R*, *red*) in hippocampus of GFAP/GSK3β. *S*, merge panel with DAPI staining in *blue*. *T* and *U*, orthogonal view of double positive NPC, which overexpress GSK3β.

carried out thymidine analog experiments. Using different thymidine analog incorporation, we checked the division cell cycle re-entry to discard differences in division speed. Thus, IdU was injected, and after 12 h, CldU was injected. The animals were sacrificed 2 h later, and the total number of double labeled NPCs was quantified (Fig. 6, *A* and *B*). No statistical differences

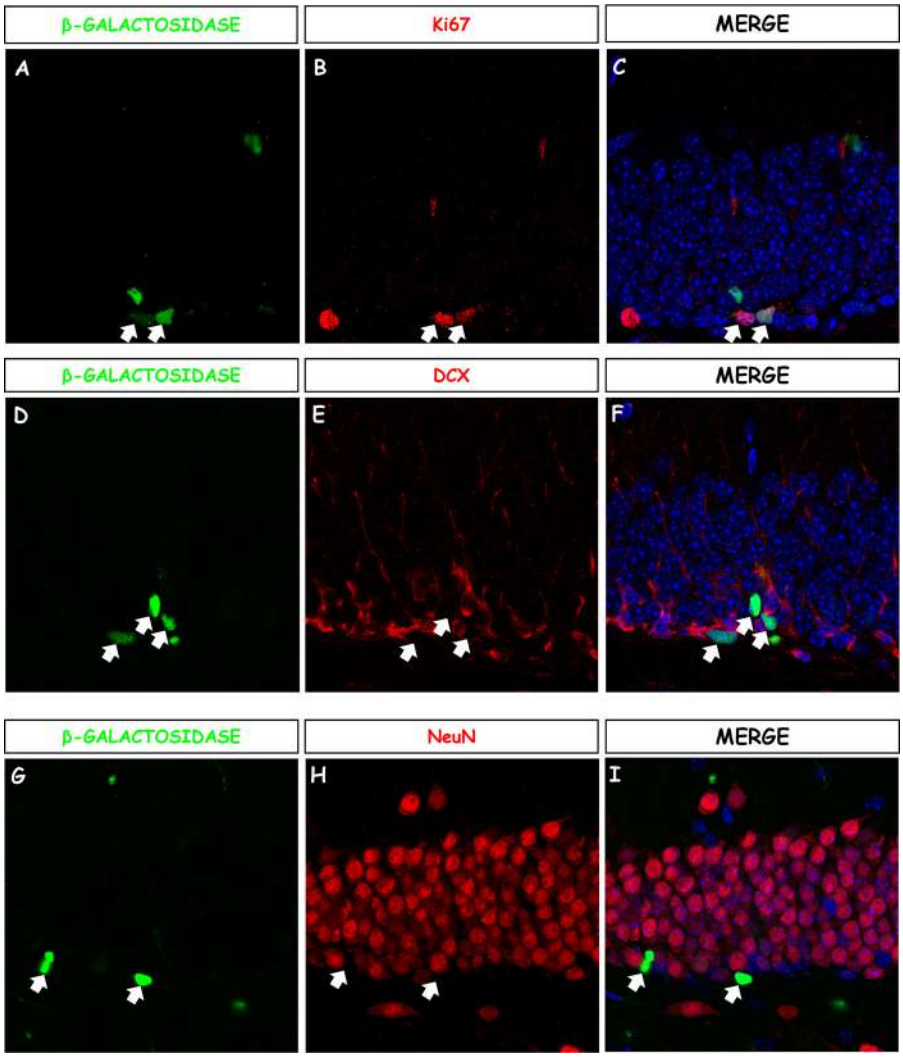

FIGURE 3. **Transgene expression in different maturation stages cells in DG.** The *left column* (*A*, *D*, and *G*; *green channel*) corresponds to β-galactosidase immunofluorescence in GFAP/GSK3β mice. The *middle column* (*B*, *E*, and *H*; *red channel*) shows Ki67 (*B*, proliferation marker), DCX (*E*, differentiation and migration marker), and NeuN (*H*, adult neurons) immunostaining. The *right column* shows merge images (*C*, *F*, and *I*) with nuclei stained with DAPI (*blue channel*). The *white arrows* in the *middle* and *right columns* show positive cells for Ki67 colocalizing with β-gal (*B* and *C*) and the lack of costaining with DCX (*E* and *F*) and NeuN (*H* and *I*) of β-gal-positive cells.

were detected between WT and GFAP/GSK3β mice (Fig. 6*C*), suggesting that in transgenic mice, an increase in re-entry into the cell cycle does not constitute a likely hypothesis.

We also carried out other kinds of experiments with thymidine analogs at different time points to check possible differences in neuronal survival caused by GSK3β overexpression. We quantified new neurons at 24 h (Fig. 6, *D* and *E*), 1 week (Fig. 6, *G* and *H*), and 4 weeks of age. In the same manner, there were not statistical differences in survival at 24 h (Fig. 6*F*), 1 week (Fig. 6*I*), or 4 weeks (Fig. 6*J*) between new cells generated in GFAP/GSK3β or in WT mice. Then we analyzed the number of DCX+ neuroblasts and the number of calbindin+ immature neurons positive for IdU (Fig. 6, *K* and *L*). We did not find statistical differences between GFAP/GSK3β mice and WT mice in Idu+DCX+ and Idu+Calbindin+, suggesting that in transgenic mice, alterations in differentiation/maturation stages do not constitute a likely hypothesis.

Then, to know whether a decrease in apoptosis might be related to the increased number of DG neurons, the death rate was evaluated by immunostaining with the anti-fractin antibody, which labels actin fragments cleaved by caspase-3 (Fig. 6*M*). As observed, the number of fractin+ cells in the SGZ was not significantly higher in GSK3β-overexpressing mice. This suggests that a decrease in apoptosis in NPCs in the adult does not likely happen in the SGZ.

Having in mind these results and the fact that the transgene is expressed in GFAP/GSK3β mice from the last stages of the embryonic period, we hypothesized that the changes observed could be produced for the effect of GSK3β overexpression in NPCs during DG formation. This structure is formed postnatally during the first month of age. Interestingly, there is a peak of expression of GSK3β, during that period after birth, when development of DG is taking place (25, 26). The overexpression of the kinase in GFAP/GSK3β mice in this period could produce an alteration of this process. To test this notion, we first tested in Nissl-stained sections from WT and GFAP/GSK3β mice whether the observed increase in adult DG volume (Fig. 4, *A*–*C*) occurred at the same grade in younger mice (Table 1).

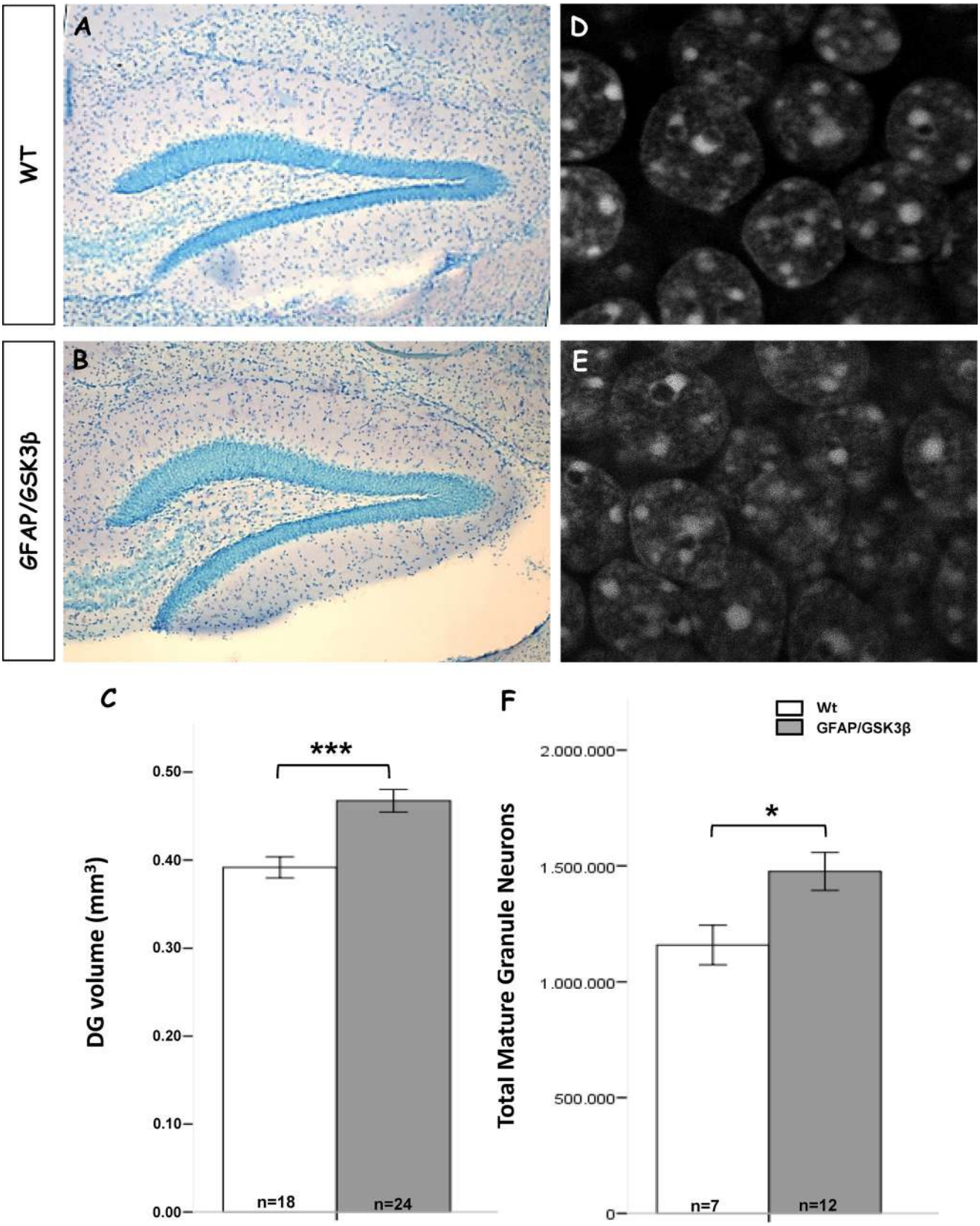

FIGURE 4. **GSK3β transgenic mice show an increase in DG volume and number of mature granule neurons.** *A* and *B*, Nissl staining to visualize cells nuclei in sagittal section of WT (*A*) and GFAP/GSK3β (*B*) mice. *C*, quantification of total DG volume expressed in mm^3 using Cavalieri method ($p = 0.0001$). *D* and *E*, mature granule neurons nuclei stained with DAPI sagittal section of WT (*D*) and GFAP/GSK3β (*E*) mice. *F*, quantification of total mature granule neurons in both genotypes ($p = 0.015$). ***, $p < 0.001$; *, $p < 0.05$. n = number of animals analyzed.

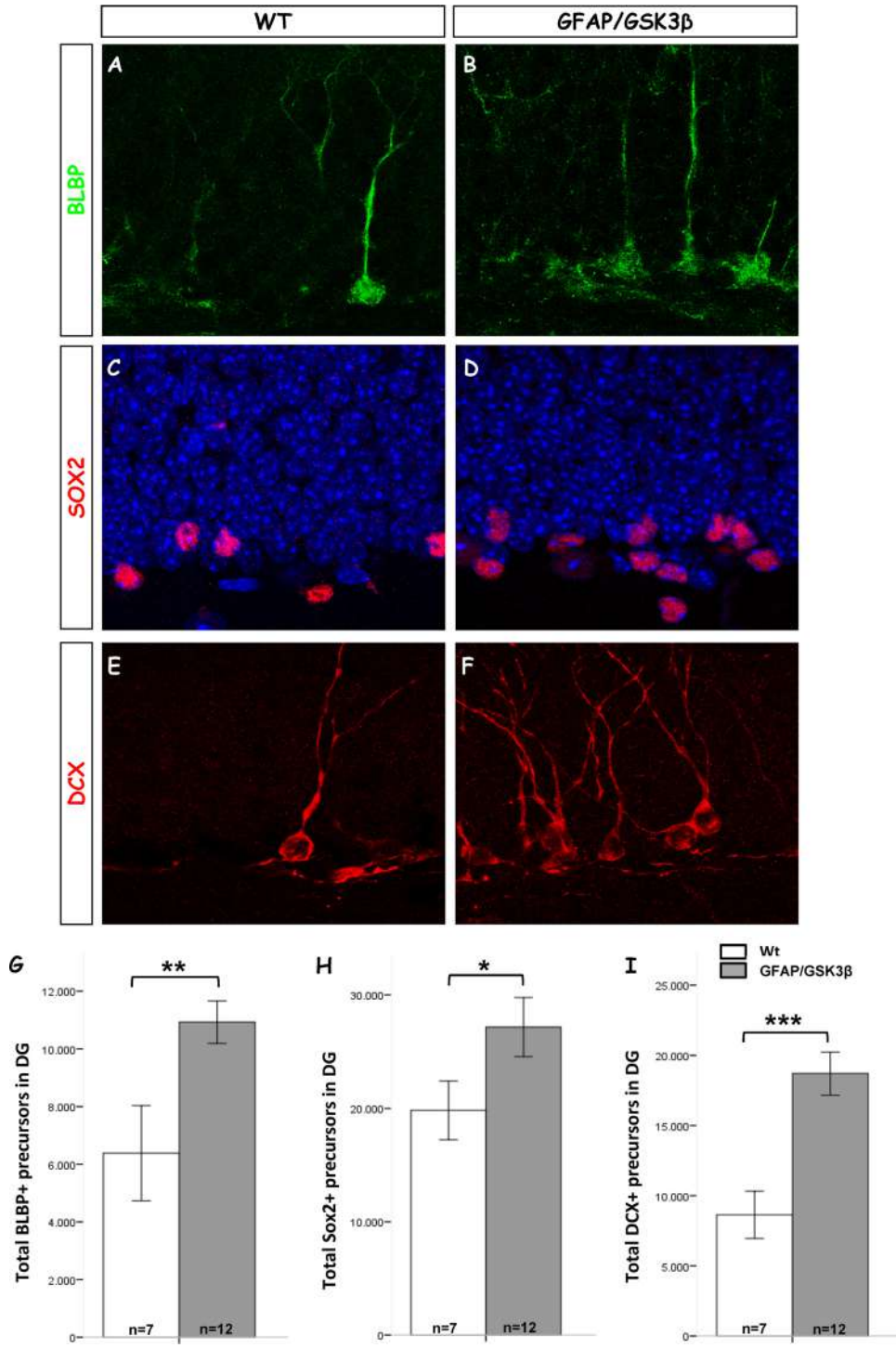

FIGURE 5. **Overexpression of GSK3β produces an increase of neural progenitors.** *A* and *B*, BLBP immunolabeling in DG of sagittal brain sections of WT mice (*A*) and GFAP/GSK3β mice (*B*). *C* and *D*, Sox2 immunolabeling in DG of sagittal brain sections of WT mice (*C*) and GFAP/GSK3β mice (*D*). *E* and *F*, DCX immunolabeling in DG of sagittal brain sections of WT mice (*E*) and GFAP/GSK3β mice (*F*). *G*, quantification of total BLBP neural progenitors ($p = 0.004$). *H*, quantification of total Sox2 neural progenitors ($p = 0.019$). *I*, quantification of total DCX neural progenitors ($p = 0.0001$). ***, $p < 0.001$; **, $p < 0.01$; *, $p < 0.05$. n = number of animals analyzed.

Quantification revealed that in young animals (14-day- and 1-month-old mice), that increase was not observed. Then we quantified the number of NPCs in 14-day-old mice (Fig. 7).

Using a physical dissector method, we estimated the amount of neural precursor by assessing the number of cells labeled with BLBP (Fig. 7, *A* and *B*) and with Sox2 (Fig. 7, *C* and *D*). With both markers we observed a statistical increase in the number of neural precursor cells in GSK3β transgenic mice compared with WT mice (Fig. 7, *G* and *H*). Then we carried out the evaluation of proliferation rate by immunolabeling using the antibody anti-phospho histone H3, a mitotic marker (Fig. 7, *E* and *F*). Statistical differences between both genotypes were observed in NPCs proliferation (Fig. 7*I*). Thus, the increase in the starting pool of NPCs when DG

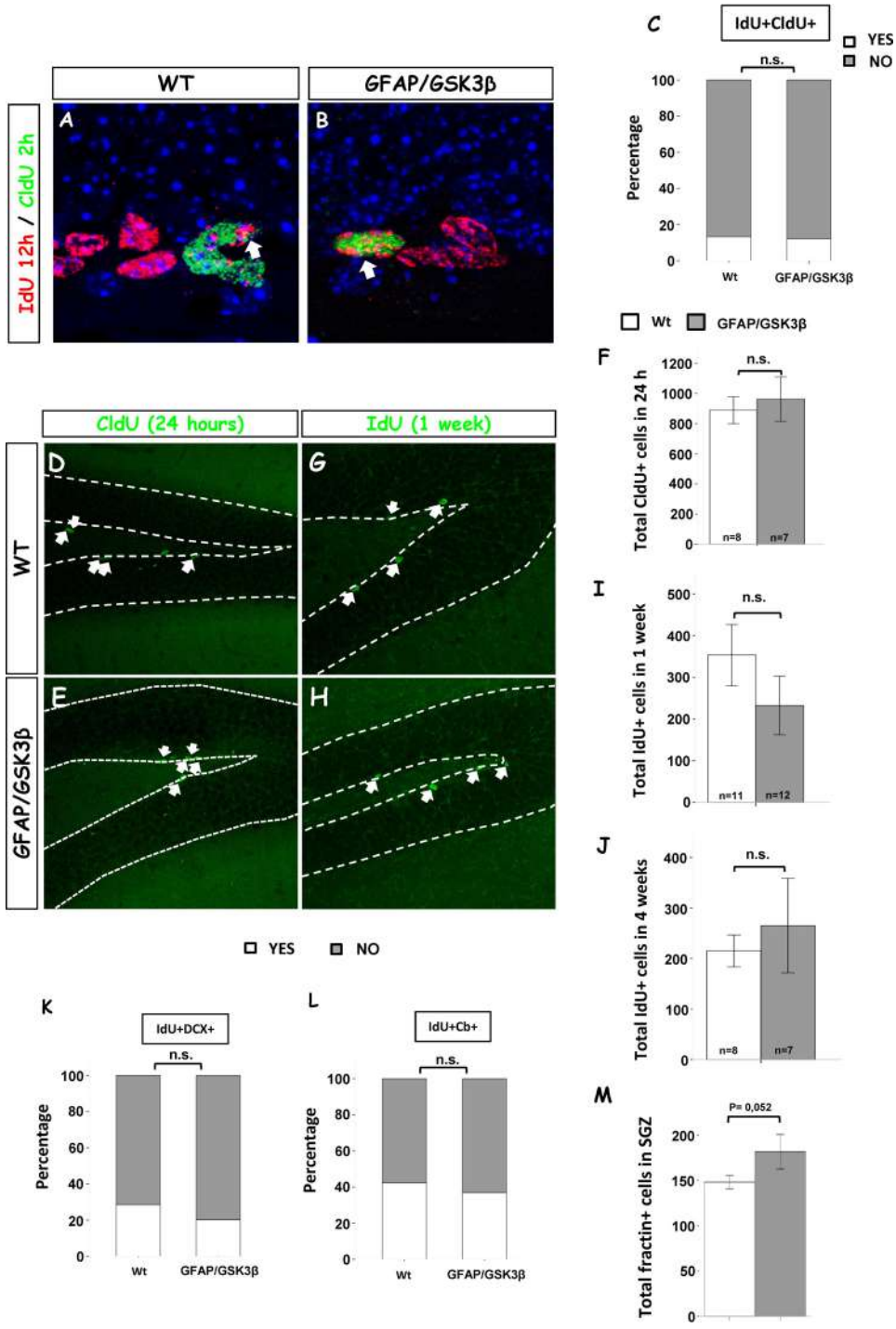

FIGURE 6. **Neural precursor cells from GSK3β-overexpressing mice do not show any alteration in cell cycle re-entry and survival.** IdU was injected, and after 12 h, CldU was injected. *A* and *B*, double immunostaining against thymidine analogs, IdU (*red channel*) and CldU (*green channel*) in WT (*A*) and GSK3β mice (*B*). The *white arrows* show positive cells for both markers. *C*, quantification of the percentage of cells labeled for both markers of the total IdU cells analyzed ($p = 0.488$). *D* and *E*, detection of CldU+ cells after 24 h postinjection in WT mice (*D*) and GFAP/GSK3β mice (*E*). *F*, quantification of the total CldU+ cells in both genotypes ($p = 1$). *G* and *H*, immunofluorescence to detect IdU+ cells after 1 week postinjection in WT mice (*G*) and GFAP/GSK3β mice (*H*). *I*, quantification of the total IdU+ cells with 1 week of age in both genotypes ($p = 0.619$). *J*, quantification of the total IdU+ cells with 4 weeks of age in both genotypes ($p = 1$). *K*, quantification of 4-week-old newborn neurons expressing DCX ($p = 0.173$). *L*, quantification of 4-week-old newborn neurons expressing Calbindin ($p = 0.427$). *M*, quantification of the total number of apoptotic cells expressing fractin. *n.s.*, no significant. *n* = number of animals analyzed.

TABLE 1

Volumetric quantification of dentate gyrus volumen of wild type and GFAP/GSK3β mice

Age	14 days	1 month	3 months
Wild type (mm^3)	0.371 ± 0.009 ($n = 7$)	0.400 ± 0.022 ($n = 7$)	0.392 ± 0.012 ($n = 18$)
GFAP-GSK3 (mm^3)	0.376 ± 0.013 ($n = 7$)	0.431 ± 0.011 ($n = 8$)	0.467 ± 0.013 ($n = 24$)
Significance (p value)	0.742	0.223	0.001

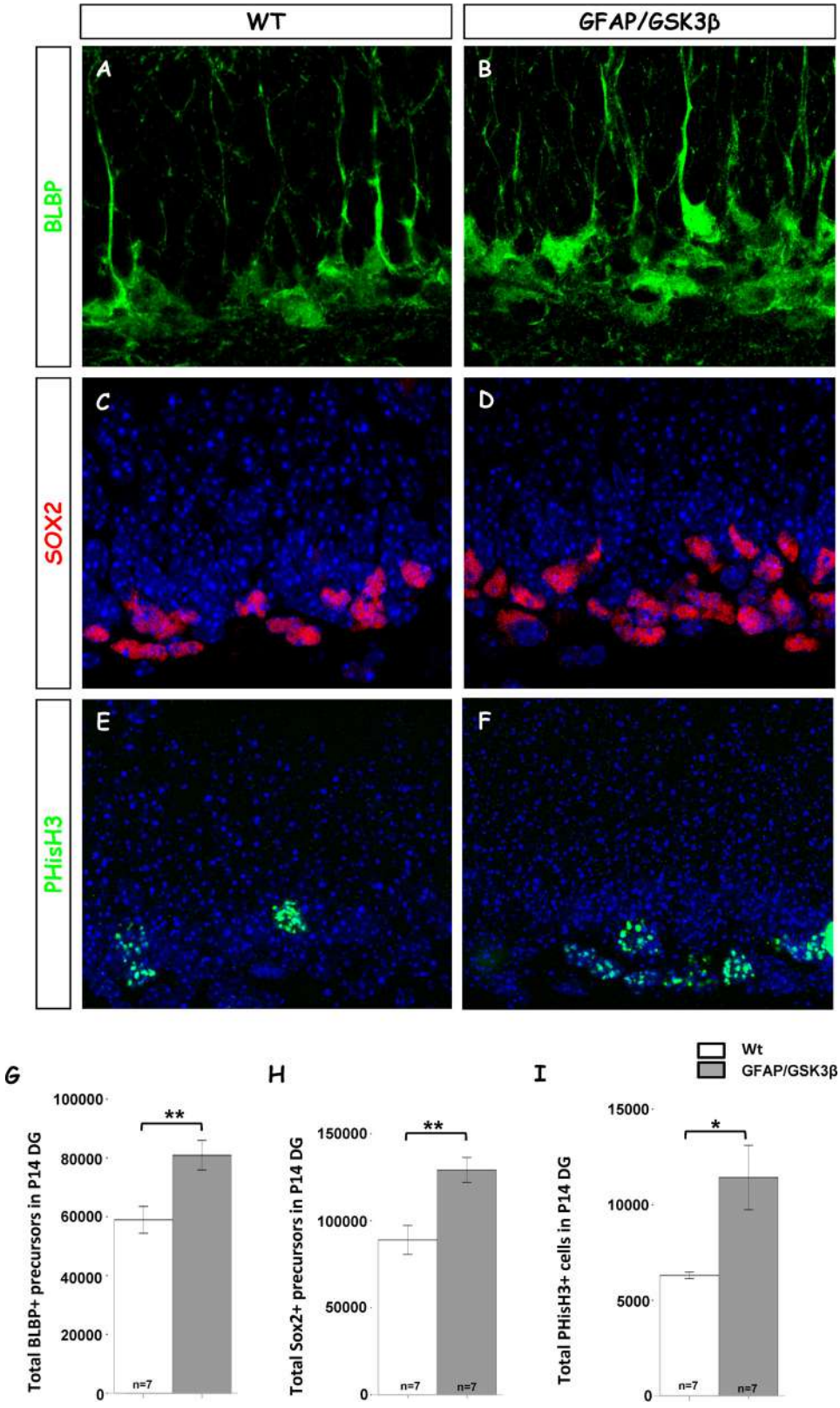

FIGURE 7. **The developing DG in P14 transgenic GSK3β mice present an increased number of neural progenitors.** *A* and *B*, BLBP immunolabeling of sagittal brain sections of P14 WT mice DG (*A*) and P14 GFAP/GSK3β mice DG (*B*). *C* and *D*, Sox2 immunolabeling in DG of sagittal brain sections of P14 WT mice DG (*C*) and P14 GFAP/GSK3β mice DG (*D*). *E* and *F*, PHisH3 immunostaining of sagittal brain sections of P14 WT mice DG (*E*) and P14 GFAP/GSK3β mice DG (*F*). *G*, quantification of total BLBP neural progenitors ($p = 0.007$). *H*, quantification of total Sox2 neural progenitors ($p = 0.003$). *I*, quantification of total PHisH3 neural progenitors ($p = 0.023$). **, $p < 0.01$; *, $p < 0.05$. n = number of animals analyzed.

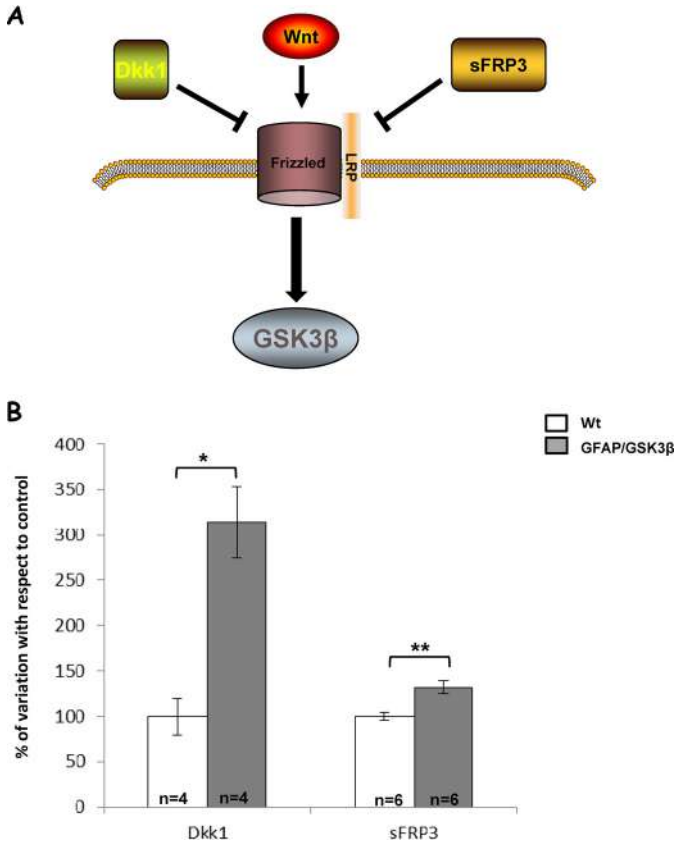

FIGURE 8. **Increase of Wnt pathway inhibitors in GFAP/GSK3β mice.** *A*, diagram of the inhibitors action on Wnt-Frizzled complex, which drives to GSK3β activity regulation. *B*, mRNA levels quantification of two Wnt-Frizzled complex inhibitors, Dkk1 and sFRP3, in WT and GFAP/GSK3β mice by quantitative RT-PCR. The levels were normalized by 18S gene levels as a control and expressed as percentages of variation respect to WT mice (Dkk1 $p = 0.029$; sFRP3 $p = 0.002$). *, $p < 0.05$; **, $p < 0.01$. n = number of animals analyzed.

formation was taking place could explain why we detect an increase of NPCs in adult mice.

However, this fact is not consistent with the lack of differences in the NPCs proliferation rate analyzed with division label antibodies (phospho histone H3) or with thymidine analog incorporation studies (Fig. 6). We reasoned that this could be due to the presence of external factors, which could slow down the proliferation in GFAP/GSK3β transgenic mice.

GFAP/GSK3β Transgenic Mice Present High Levels of Wnt Inhibitors—A decrease of neurogenesis is well stablished in the elderly (27–29), and recently the Wnt pathway inhibitor Dickkopf 1 (Dkk1) was proposed as an effector of that decrease (30) (Fig. 8*A*). On the other hand, during physical exercise, an increase in neurogenesis occurs (31, 32), and this effect has been attributed to the decreased levels of another Wnt pathway inhibitor, secreted frizzled-related protein 3 (sFRP3) (33) (Fig. 8*A*). Thus, we tested the possibility that both secreted factors were altered in GFAP/GSK3β mice brain. Using quantitative PCR, we found a statistically significant increase in mRNA levels of these secreted factors in GFAP/GSK3β compared with control mice (Fig. 8*B*), suggesting that high levels of Wnt-frizzled complex inhibitors could act in a compensatory manner, decreasing the expected proliferation based in the increase of progenitor cells.

Behavioral Alteration in GFAP/GSK3β Mice—As we described above, GSK3β overexpression in NPCs produces a subsequent increase of neural progenitors in GFAP/GSK3β mice. To check whether that increase has any behavioral effect, we tested transgenic and control mice in different behavioral paradigms. First, we checked mice in a general locomotion and behavioral test, such as open field test. After 15 min in the arena, the analysis of different parameters registered by the apparatus showed no differences in the general exploratory behavior of transgenic mice respect to WT. In this sense, GSK3β-overexpressing mice showed the same values in different parameters such as the total amount of vertical counts and jumps and the same average velocity (Fig. 9*A*).

Taking into account that GSK3β overexpression in NPCs produces an alteration in hippocampal neurogenesis, we challenged the animals in a hippocampus-dependent task, like a fear conditioning test. After a training day, the percentage of immobility or freezing was indicative of ambient remembering dependent on the hippocampus. The data showed a significant increase in freezing time of GFAP/GSK3β-overexpressing mice compared with WT mice (Fig. 9*B*). Thus, in a hippocampus-dependent memory test, behavioral differences were observed.

Discussion

The development of the brain requires the decision of precursors to proliferate or differentiate. Different structures are made at different times during development. Adult neurogenesis takes place in the DG, a postnatal developed structure. At approximately P4, a DG primordium can be visualized, and at that time an increase in the proliferation of neuronal cells occurs. At day 14, the shape is that of a mature DG but smaller, and the maturation finished at approximately P21. During that stage, changes in GSK3β takes place. Thus, an increase in GSK3β levels during this period of intense neurite outgrowth, but also cell division, is observed (25, 26). When DG structure is finished, a decrease in GSK3β levels occurs, and proper adult neurogenesis takes place. In this process, astrocyte-like stem cells start to proliferate. In this work, we have tested the effect of GSK3β overexpression specifically in those astrocyte-like cells.

GSK3β Overexpression in NPCs—Inhibition of the GSK3 has been associated with the maintenance of the pluripotent state in embryonic stem cells (34, 35). Thus, it has been suggested that GSK3 acts as a kinase of integration because of its essential role in Wnt3 signaling (36). The Wnt transduction pathway involves inhibition of GSK3β, which causes an increase in the levels of β-catenin and consequent activation of promoters implicated in proliferation and maintenance of pluripotent stem cells present in the SGZ. The importance of that route in this structure is reflected by the fact that the hippocampus is missing in a Wnt-3a deficient mouse (37). In good correlation, overexpression of β-catenin (38), as well as knock-out of GSK3 in neural progenitors (13), results in a massive hyperproliferation. However, other studies suggest that Wnt decreases the number neurospheres and leads to neuronal differentiation (39–42). To further complicate the scenario, the response of neural progenitors appears to depend on the levels of GSK3. Thus, the cellular decision of these cells to differentiate or to split depends largely on levels of GSK3 activity (19).

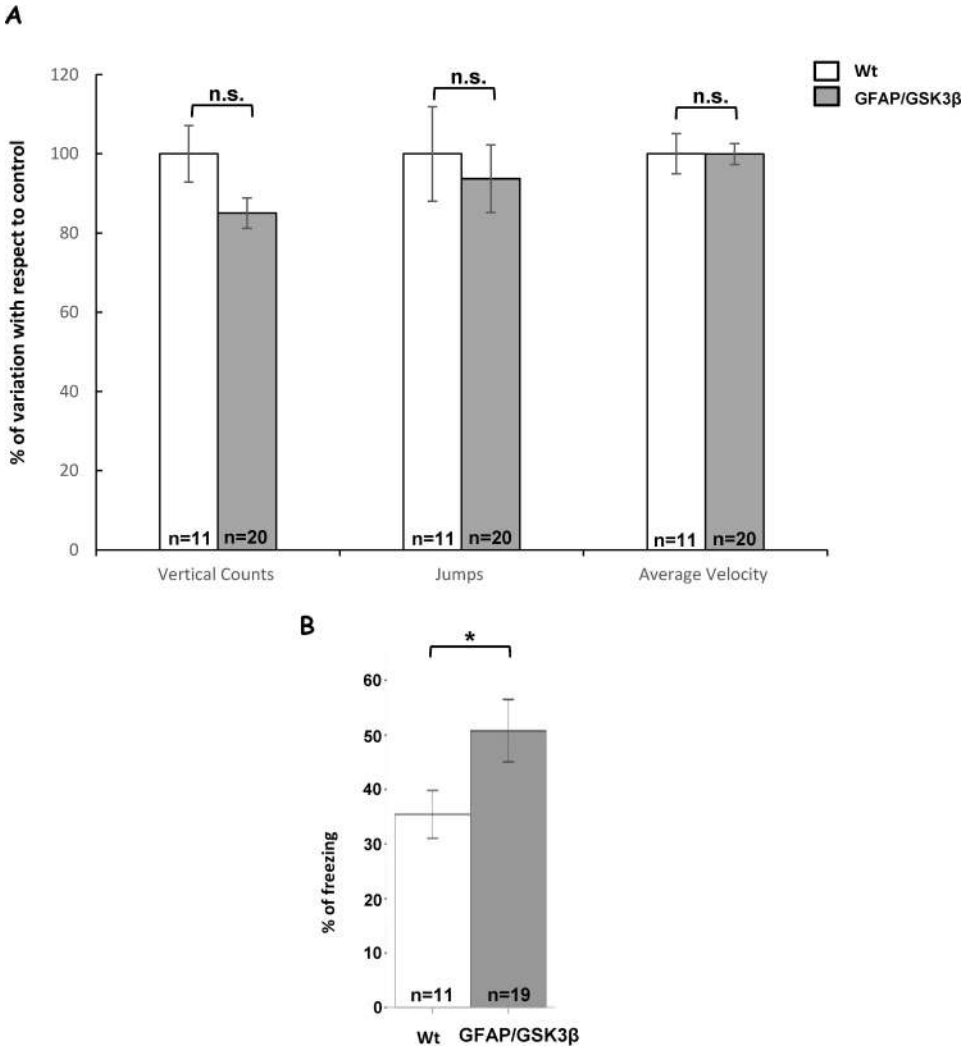

FIGURE 9. **Behavioral alteration in GFAP/GSK3β mice.** *A*, quantification of open field behavioral test perform in 15-week-old WT and GFAP/GSK3β mice. The results are expressed as percentages (vertical counts $p = 0.083$; jumps $p = 0.668$; average velocity $p = 0{,}990$). *B*, quantification of fear conditioning test carried out in 15-week-old WT and GFAP/GSK3β mice. The results are expressed as percentages of immobility time ("freezing") ($p = 0.043$). *, $p < 0.05$. *n.s.*, no significant. n = number of animals analyzed.

Most of the studies described above have been developed either in cell cultures or in animal models based primarily on the generation of animals deficient in some of the proteins involved in the transduction of Wnt. However, taking into account that NPCs progressively generate more differentiated progeny that eventually mature into granule neurons, the role of GSK3β in adult neurogenesis should be analyzed step by step. In previous reports, we found that the overexpression of the kinase in later stages of neurogenesis from DCX cells to mature neurons has negative consequences for the neurogenic process (14, 20). However, the direct role of GSK3β overexpression in the first step of the process *in vivo*, just in NPCs, has not been addressed so far.

To this end, we have expressed GSK3β gene under a GFAP promoter. GFAP is not only expressed in NPC; it can be found in many types of glial cells. However, in GFAP/GSK3β mice, a particular pattern of GFAP expression is observed because of the use of a truncated promoter. The promoter consists of a 2.2-kb human GFAP promoter adjacent to the starting codon of the protein (43). This fragment seems to determine the expression in a restricted subset of cells, agreeing with other models generated with this GFAP promoter fragment (24, 44). In this sense, full-length GFAP promoter has different regulator regions far from starting codon that regulate protein expression in other cell type like Schwann cells. These regions are missing in GFAP/GSK3β mice, and in fact no peripheral nervous system expression is seen in our model (24). Moreover, the response of GFAP transcription in a reactive gliosis is regulated at the promoter level. A fragment missed in GFAP-tTa promoter and located 13.2 kb upstream of the starting codon is responsible of a stronger gliosis response (45). This could be the reason, because transgene expression is not observed in the glial scar generated after stereotaxic injection (data not shown). Related to mature astrocytes, no wide expression of the transgene in them is detected. However, some dispersed labeling (S100β+) can be seen corresponding to some mature astrocytes.

Expression of endogenous GFAP starts in mouse in the last days of the embryonic period (embryonic days 17 and 18) when glial cells exchange the expression of vimentin for GFAP. The

GFAP expression increases from birth, reaching the highest levels between days 8 and 10 (46). GFAP/GSK3β transgenic mice show an increase of NPCs present in the immature DG (14 days after birth). These data suggest that increasing levels of GSK3β produce an expansion of neural precursor cells pool during DG development. That expansion likely is responsible for the increase in NPCs and in DG volume observed in the adult mice.

Thus, the main findings observed in GFAP/GSK3β mice, a greater number of neural progenitors BLBP- and Sox2-positive together with a greater volume of the DG accompanied by an increase in granular neurons, seem to suggest that an increase of GSK3 activity is important in the generation of new neurons and, more important, for a better performance in a hippocampus-dependent task such as a fear conditioning test. Interestingly, our results mirror, to some extent, what is happening in the development of the DG. This structure presents a fundamentally postnatal development, and it is in that period when GSK3 levels reach higher values in the central nervous system (25, 26). In fact, GSK3β enzyme, but not the α isoform, has a peak at 2 weeks, a period of intense neurite outgrowth, but also cell division, at least in the DG.

Possible Mechanisms for GSK3β Regulation of NPCs in SGZ—Taking into account all previous data, a likely mechanism by which GSK3β could regulate neurogenesis in GFAP/GSK3β mice would be by controlling levels of the molecules that are involved in neurogenesis, mainly β-catenin in the Wnt pathway (for a revision see Ref. 47). This assumption rests on the finding that during the asymmetric cell division, β-catenin phosphorylated by GSK3β is mainly inherited by one daughter cell (48). We hypothesized that increased levels of GSK3β in NPCs could produce the lack of asymmetrical protein distribution during precursor division, leading to progenitor pool expansion. It has been reported that Wnt proteins are necessary to maintain pluripotency and self-renewal of stem cells (47–49). During precursor cell division, the asymmetrical distribution of proteins of Wnt pathway determines which daughter cell will remain as a precursor cell (50). Therefore, it is possible that during the asymmetric division of neuronal progenitors, the two daughter cells have different levels of GSK3. Thus, in the asymmetric division that takes place in neural progenitors, daughter cells with lower GSK3 activity accumulate β-catenin (and perhaps other proproliferative proteins) and therefore continue to be stem cells. Conversely, the daughter cell with greater GSK3 activity eliminates pro-proliferative proteins and differentiates. In GFAP/GSK3β mice, the high levels of GSK3β overexpression obtained in NPCs could mask the polarized distribution of Wnt proteins. As a result, in both daughter cells high levels of GSK3 will exist, β avoiding the effect of this asymmetrical distribution in precursors division. Thus, the division of a GFAP stem cell will produce two more linage-restricted cells (rapid amplifying cells) characterized by Sox2 and BLBP markers. This fact could explain the reported increased number of NPCs in GSK3β transgenic mice, although some experiments will be necessary to really confirm this hypothesis.

Another possible hypothesis that could explain the observed increase of NPCs in adult transgenic mice would be an increase in precursor cells proliferation. More proliferation events would be expected if more precursor cells are present, but no differences in mitosis rate were detected in GFAP/GSK3β-overexpressing mice. Interestingly, an increase in apoptosis was also not observed. The explanation for this phenomenon could be the increased levels of Dkk1 and sFRP3, two Wnt-Frizzled inhibitors (30, 33). These molecules inactivate the Wnt pathway with the subsequent increase in β-catenin degradation and reduction of the expression of proneurogenic genes. GFAP/GSK3β mice show high mRNA levels of Dkk1 and sFRP3, in a likely attempt to keep the enhanced pool of NPCs controlled and avoid and excess of neurogenesis.

In summary, in this work we have analyzed the consequences of GSK3β overexpression in NPCs. We have found increases in NPCs and DG volume and an improvement in memory skills. In previous studies, it was demonstrated that overexpression of GSK3β under CamkII promoter (14, 20), a late promoter that is expressed in immature neurons, results in cell death, memory impairment and a decrease in DG volume Thus, it seems that during neurogenesis, changes in the levels of GSK3β occur, and they are needed to carry out the process in a proper way. Accordingly, to maintain the pluripotency state a decrease in GSK3 activity is necessary, whereas an increase in GSK3 activity seems to be necessary during asymmetric division of neuronal precursors to initiate differentiation.

Author Contributions—J. J.-A. performed the experiments. J. J.-A. and M. L.-M. analyzed the data. F. H. and J. A. designed the study and wrote the paper. All authors approved the final version of the manuscript.

References

1. Eriksson, P. S., Perfilieva, E., Björk-Eriksson, T., Alborn, A. M., Nordborg, C., Peterson, D. A., and Gage, F. H. (1998) Neurogenesis in the adult human hippocampus. *Nat. Med.* **4,** 1313–1317
2. Altman, J., and Das, G. D. (1965) Post-natal origin of microneurones in the rat brain. *Nature* **207,** 953–956
3. Altman, J., and Das, G. D. (1965) Autoradiographic and histological evidence of postnatal hippocampal neurogenesis in rats. *J. Comp. Neurol.* **124,** 319–335
4. Doetsch, F., Caillé, I., Lim, D. A., García-Verdugo, J. M., and Alvarez-Buylla, A. (1999) Subventricular zone astrocytes are neural stem cells in the adult mammalian brain. *Cell* **97,** 703–716
5. Seri, B., García-Verdugo, J. M., McEwen, B. S., and Alvarez-Buylla, A. (2001) Astrocytes give rise to new neurons in the adult mammalian hippocampus. *J. Neurosci.* **21,** 7153–7160
6. Bayer, S. A., and Altman, J. (1974) Hippocampal development in the rat: cytogenesis and morphogenesis examined with autoradiography and low-level X-irradiation. *J. Comp. Neurol.* **158,** 55–79
7. Altman, J., and Bayer, S. A. (1990) Migration and distribution of two populations of hippocampal granule cell precursors during the perinatal and postnatal periods. *J. Comp. Neurol.* **301,** 365–381
8. Altman, J., and Bayer, S. A. (1990) Mosaic organization of the hippocampal neuroepithelium and the multiple germinal sources of dentate granule cells. *J. Comp. Neurol.* **301,** 325–342
9. Bayer, S. A., Yackel, J. W., and Puri, P. S. (1982) Neurons in the rat dentate gyrus granular layer substantially increase during juvenile and adult life. *Science* **216,** 890–892
10. van Praag, H., Schinder, A. F., Christie, B. R., Toni, N., Palmer, T. D., and Gage, F. H. (2002) Functional neurogenesis in the adult hippocampus. *Nature* **415,** 1030–1034
11. Aimone, J. B., Li, Y., Lee, S. W., Clemenson, G. D., Deng, W., and Gage, F. H. (2014) Regulation and function of adult neurogenesis: from genes to

cognition. *Physiol. Rev.* **94,** 991–1026
12. Eom, T. Y., and Jope, R. S. (2009) Blocked inhibitory serine-phosphorylation of glycogen synthase kinase-3α/β impairs in vivo neural precursor cell proliferation. *Biol. Psychiatry* **66,** 494–502
13. Kim, W. Y., Wang, X., Wu, Y., Doble, B. W., Patel, S., Woodgett, J. R., and Snider, W. D. (2009) GSK-3 is a master regulator of neural progenitor homeostasis. *Nat. Neurosci.* **12,** 1390–1397
14. Fuster-Matanzo, A., Llorens-Martín, M., Sirerol-Piquer, M. S., García-Verdugo, J. M., Avila, J., and Hernández, F. (2013) Dual effects of increased glycogen synthase kinase-3β activity on adult neurogenesis. *Hum. Mol. Genet.* **22,** 1300–1315
15. Sirerol-Piquer, M., Gomez-Ramos, P., Hernández, F., Perez, M., Morán, M. A., Fuster-Matanzo, A., Lucas, J. J., Avila, J., and García-Verdugo, J. M. (2011) GSK3β overexpression induces neuronal death and a depletion of the neurogenic niches in the dentate gyrus. *Hippocampus* **21,** 910–922
16. Beurel, E., Grieco, S. F., and Jope, R. S. (2015) Glycogen synthase kinase-3 (GSK3): regulation, actions, and diseases. *Pharmacol. Ther.* **148,** 114–131
17. Kim, W. Y., and Snider, W. D. (2011) Functions of GSK-3 signaling in development of the nervous system. *Front. Mol. Neurosci.* **4,** 44
18. Mao, Y., Ge, X., Frank, C. L., Madison, J. M., Koehler, A. N., Doud, M. K., Tassa, C., Berry, E. M., Soda, T., Singh, K. K., Biechele, T., Petryshen, T. L., Moon, R. T., Haggarty, S. J., and Tsai, L. H. (2009) Disrupted in schizophrenia 1 regulates neuronal progenitor proliferation via modulation of GSK3β/β-catenin signaling. *Cell* **136,** 1017–1031
19. Holowacz, T., Alexson, T. O., Coles, B. L., Doble, B. W., Kelly, K. F., Woodgett, J. R., and Van Der Kooy, D. (2013) The responses of neural stem cells to the level of GSK-3 depend on the tissue of origin. *Biol. Open.* **2,** 812–821
20. Llorens-Martín, M., Fuster-Matanzo, A., Teixeira, C. M., Jurado-Arjona, J., Ulloa, F., Defelipe, J., Rábano, A., Hernández, F., Soriano, E., and Avila, J. (2013) Alzheimer disease-like cellular phenotype of newborn granule neurons can be reversed in GSK-3β-overexpressing mice. *Mol. Psychiatry* **18,** 395
21. Lucas, J. J., Hernández, F., Gómez-Ramos, P., Morán, M. A., Hen, R., and Avila, J. (2001) Decreased nuclear β-catenin, Tau hyperphosphorylation and neurodegeneration in GSK-3β conditional transgenic mice. *EMBO J.* **20,** 27–39
22. Llorens-Martín, M., Tejeda, G. S., and Trejo, J. L. (2010) Differential regulation of the variations induced by environmental richness in adult neurogenesis as a function of time: a dual birthdating analysis. *PLoS One* **5,** e12188
23. Llorens-Martín, M., Torres-Alemán, I., and Trejo, J. L. (2006) Pronounced individual variation in the response to the stimulatory action of exercise on immature hippocampal neurons. *Hippocampus* **16,** 480–490
24. Lin, W., Kemper, A., McCarthy, K. D., Pytel, P., Wang, J. P., Campbell, I. L., Utset, M. F., and Popko, B. (2004) Interferon-γ induced medulloblastoma in the developing cerebellum. *J. Neurosci.* **24,** 10074–10083
25. Takahashi, M., Tomizawa, K., and Ishiguro, K. (2000) Distribution of Tau protein kinase I/glycogen synthase kinase-3β, phosphatases 2A and 2B, and phosphorylated Tau in the developing rat brain. *Brain Res.* **857,** 193–206
26. Yu, Y., Run, X., Liang, Z., Li, Y., Liu, F., Liu, Y., Iqbal, K., Grundke-Iqbal, I., and Gong, C. X. (2009) Developmental regulation of Tau phosphorylation, Tau kinases, and Tau phosphatases. *J. Neurochem.* **108,** 1480–1494
27. Seki, T., and Arai, Y. (1995) Age-related production of new granule cells in the adult dentate gyrus. *Neuroreport* **6,** 2479–2482
28. Kuhn, H. G., Dickinson-Anson, H., and Gage, F. H. (1996) Neurogenesis in the dentate gyrus of the adult rat: age-related decrease of neuronal progenitor proliferation. *J. Neurosci.* **16,** 2027–2033
29. Kempermann, G., Kuhn, H. G., and Gage, F. H. (1998) Experience-induced neurogenesis in the senescent dentate gyrus. *J. Neurosci.* **18,** 3206–3212
30. Jang, M. H., Bonaguidi, M. A., Kitabatake, Y., Sun, J., Song, J., Kang, E., Jun, H., Zhong, C., Su, Y., Guo, J. U., Wang, M. X., Sailor, K. A., Kim, J. Y., Gao, Y., Christian, K. M., Ming, G. L., and Song, H. (2013) Secreted frizzled-related protein 3 regulates activity-dependent adult hippocampal neurogenesis. *Cell Stem Cell* **12,** 215–223
31. van Praag, H., Kempermann, G., and Gage, F. H. (1999) Running increases cell proliferation and neurogenesis in the adult mouse dentate gyrus. *Nat. Neurosci.* **2,** 266–270
32. van Praag, H., Christie, B. R., Sejnowski, T. J., and Gage, F. H. (1999) Running enhances neurogenesis, learning, and long-term potentiation in mice. *Proc. Natl. Acad. Sci. U.S.A.* **96,** 13427–13431
33. Seib, D. R., Corsini, N. S., Ellwanger, K., Plaas, C., Mateos, A., Pitzer, C., Niehrs, C., Celikel, T., and Martin-Villalba, A. (2013) Loss of Dickkopf-1 restores neurogenesis in old age and counteracts cognitive decline. *Cell Stem Cell* **12,** 204–214
34. Miki, T., Yasuda, S. Y., and Kahn, M. (2011) Wnt/β-catenin signaling in embryonic stem cell self-renewal and somatic cell reprogramming. *Stem Cell Rev.* **7,** 836–846
35. Sato, N., Meijer, L., Skaltsounis, L., Greengard, P., and Brivanlou, A. H. (2004) Maintenance of pluripotency in human and mouse embryonic stem cells through activation of Wnt signaling by a pharmacological GSK-3-specific inhibitor. *Nat. Med.* **10,** 55–63
36. Okamoto, M., Inoue, K., Iwamura, H., Terashima, K., Soya, H., Asashima, M., and Kuwabara, T. (2011) Reduction in paracrine Wnt3 factors during aging causes impaired adult neurogenesis. *FASEB J.* **25,** 3570–3582
37. Lee, S. M., Tole, S., Grove, E., and McMahon, A. P. (2000) A local Wnt-3a signal is required for development of the mammalian hippocampus. *Development* **127,** 457–467
38. Chenn, A., and Walsh, C. A. (2002) Regulation of cerebral cortical size by control of cell cycle exit in neural precursors. *Science* **297,** 365–369
39. Hirabayashi, Y., Itoh, Y., Tabata, H., Nakajima, K., Akiyama, T., Masuyama, N., and Gotoh, Y. (2004) The Wnt/β-catenin pathway directs neuronal differentiation of cortical neural precursor cells. *Development* **131,** 2791–2801
40. Kuwahara, A., Hirabayashi, Y., Knoepfler, P. S., Taketo, M. M., Sakai, J., Kodama, T., and Gotoh, Y. (2010) Wnt signaling and its downstream target N-myc regulate basal progenitors in the developing neocortex. *Development* **137,** 1035–1044
41. Muroyama, Y., Kondoh, H., and Takada, S. (2004) Wnt proteins promote neuronal differentiation in neural stem cell culture. *Biochem. Biophys. Res. Commun.* **313,** 915–921
42. Munji, R. N., Choe, Y., Li, G., Siegenthaler, J. A., and Pleasure, S. J. (2011) Wnt signaling regulates neuronal differentiation of cortical intermediate progenitors. *J. Neurosci.* **31,** 1676–1687
43. Besnard, F., Brenner, M., Nakatani, Y., Chao, R., Purohit, H. J., and Freese, E. (1991) Multiple interacting sites regulate astrocyte-specific transcription of the human gene for glial fibrillary acidic protein. *J. Biol. Chem.* **266,** 18877–18883
44. Weber, T., Baier, V., Pauly, R., Sahay, A., Baur, M., Herrmann, E., Ciccolini, F., Hen, R., Kronenberg, G., and Bartsch, D. (2011) Inducible gene expression in GFAP+ progenitor cells of the SGZ and the dorsal wall of the SVZ-A novel tool to manipulate and trace adult neurogenesis. *Glia* **59,** 615–626
45. Mucke, L., Oldstone, M. B., Morris, J. C., and Nerenberg, M. I. (1991) Rapid activation of astrocyte-specific expression of GFAP-lacZ transgene by focal injury. *New. Biol.* **3,** 465–474
46. Kim, J. S., Kim, J., Kim, Y., Yang, M., Jang, H., Kang, S., Kim, J. C., Kim, S. H., Shin, T., and Moon, C. (2011) Differential patterns of nestin and glial fibrillary acidic protein expression in mouse hippocampus during postnatal development. *J. Vet. Sci.* **12,** 1–6
47. Hur, E. M., and Zhou, F. Q. (2010) GSK3 signalling in neural development. *Nat. Rev. Neurosci.* **11,** 539–551
48. Fuentealba, L. C., Eivers, E., Geissert, D., Taelman, V., and De Robertis, E. M. (2008) Asymmetric mitosis: unequal segregation of proteins destined for degradation. *Proc. Natl. Acad. Sci. U.S.A.* **105,** 7732–7737
49. ten Berge, D., Kurek, D., Blauwkamp, T., Koole, W., Maas, A., Eroglu, E., Siu, R. K., and Nusse, R. (2011) Embryonic stem cells require Wnt proteins to prevent differentiation to epiblast stem cells. *Nat. Cell Biol.* **13,** 1070–1075
50. Yamashita, Y. M., Jones, D. L., and Fuller, M. T. (2003) Orientation of asymmetric stem cell division by the APC tumor suppressor and centrosome. *Science* **301,** 1547–1550

GSK3β Overexpression in Dentate Gyrus Neural Precursor Cells Expands the Progenitor Pool and Enhances Memory Skills

Jerónimo Jurado-Arjona, María Llorens-Martín, Jesús Ávila and Félix Hernández

J. Biol. Chem. 2016, 291:8199-8213.
doi: 10.1074/jbc.M115.674531 originally published online February 17, 2016
